Eur. Phys. J. A (2013) **49**: 109
DOI 10.1140/epja/i2013-13109-5

THE EUROPEAN PHYSICAL JOURNAL A

Regular Article – Experimental Physics

Decay of ^{185}Tl, $^{185m+g}$Hg, $^{189m+g}$Pb and energy location of the $13/2^+$ isomeric states in ^{185}Hg, ^{189}Pb, ^{193}Po and ^{197}Rn

J. Sauvage[1,a], B. Roussière[1], J. Genevey[2], S. Franchoo[1], A.N. Andreyev[3], N. Barre[1], A. Ben Braham[4], C. Bourgeois[1], J.-F. Clavelin[1], H. De Witte[5], D.V. Fedorov[6], V.N. Fedoseyev[7], L.M. Fraile[8], X. Grave[1], G. Huber[9], M. Huyse[5], P. Kilcher[1], U. Köster[10], P. Kunz[11], S.R. Lesher[12], B.A. Marsh[7], I. Mukha[5], J. Oms[1], M.G. Porquet[13], M. Seliverstov[6,9], I. Stefanescu[14], K. Van de Vel[5], P. Van Duppen[5], YU.M. Volkov[6], and A. Wojtasiewicz[15]

[1] Institut de Physique Nucleaire, IN2P3-CNRS/Université Paris-Sud, F-91406 Orsay Cedex, France
[2] Laboratoire de Physique Subatomique et de Cosmologie, IN2P3-CNRS/Universite Joseph Fourier, F-38026 Grenoble Cedex, France
[3] Department of Physics, University of York, York, YO10 5DD, UK
[4] Faculté des sciences de Tunis, 1060 le Belvédère, Tunis, Tunisia
[5] Instituut voor Kern- en Stralingsfysica, K.U. Leuven, B-3001 Leuven, Belgium
[6] Petersburg Nuclear Physics Institute, 188350, Gatchina, Russia
[7] ISOLDE, CERN, CH-1211 Genève 23, Switzerland
[8] Grupo de Fisica Nuclear, Universidad Complutense, CEI Moncloa, 28040 Madrid, Spain
[9] Institut für Physik, Johannes Gutenberg Universität, D-55099 Mainz, Germany
[10] Institut Laue-Langevin, F-38042 Grenoble Cedex 9, France
[11] TRIUMF, Vancouver BC, V6T 2A3, Canada
[12] University of Wisconsin-La Crosse, La Crosse, WI 54601, USA
[13] Centre de Sciences Nucléaires et de Sciences de la Matière, F-91405 Orsay, France
[14] Forschungs-Neutronenquelle Heinz Maier-Leibnitz, Technische Universität München, D-85748 Garching, Germany
[15] Institute of Experimental Physics, University of Warsaw, Warsaw, Poland

Received: 17 December 2012 / Revised: 5 July 2013
Published online: 6 September 2013
© The Author(s) 2013. This article is published with open access at Springerlink.com
Communicated by J. Äystö

Abstract. The β^+/EC decay of ^{185}Tl was studied at the ISOLDE facility, the γ-rays belonging to ^{185}Hg have been identified and a partial low-spin level scheme of ^{185}Hg has been built. The decay of $^{185m+g}$Hg was studied at the ISOCELE facility. Conversion electron lines of very low-energy transitions were observed for the first time. Electron data have been obtained for four transitions in ^{185}Au and two transitions in ^{185}Hg. From the analysis performed using an internal energy calibration procedure the energy location of the ^{185m}Hg has been determined to be $E_{IS} = 103.7(4)$ keV. This E_{IS} value is consistent with that determined independently, $E_{IS} = 94(13)$ keV, using $^{185m+g}$Hg α-decay data from literature. New α particles emitted from $^{189m+g}$Pb have been detected and their origins determined by in-source laser spectroscopy at the ISOLDE facility. α-γ coincidence results have served to locate the $13/2^+$ isomeric state of ^{189}Pb at $E_{IS} = 40(4)$ keV. This latter E_{IS} value added to α-decay data from literature have allowed the energy location of the $13/2^+$ isomeric states of ^{193}Po and ^{197}Rn at 95(7) keV and 194(12) keV, respectively. The nuclear structure of the isomeric and ground states in the nuclei of the three α-emitter chains starting with $^{195m+g,197m+g,199m+g}$Rn are discussed.

1 Introduction

Atomic and nuclear spectroscopy studies have revealed great nuclear-shape instability for the neutron-deficient Hg, Au, Pt and Ir nuclei situated far from the valley of stability. For these elements, states corresponding to a rather large nuclear deformation appear suddenly for a mass number $A < 187$ [1–7], giving rise to shape or deformation change between neighbouring isotopes and/or to coexistence of states having different nuclear shapes or deformations in one nucleus. The most spectacular examples of shape coexistence have been discovered in the ^{185,186}Hg nuclei where states corresponding to very different deformation parameters, $|\beta| = 0.15$ and $\beta = 0.25$, coexist at low excitation energy [1,2]. These phenomena

[a] e-mail: sauvage@ipno in2p3 fr

caused a large interest and numerous experimental and theoretical works have been performed [8–10]. In recent years, the deformation evolution of the neutron-deficient $^{182-190}$Pb nuclei was investigated by in-source laser spectroscopy. The changes in nuclear charge radius and the nuclear-moment values have already been published [11, 12]. These results have shown that the Pb nuclei in their isomeric and ground states keep a quasi-spherical shape even far from the valley of stability. New α particles emitted from the $^{189m+g}$Pb nucleus have been detected during the latter experiment. They can serve to determine the energy location of the $13/2^+$ isomeric state of the ^{189}Pb nucleus provided the energy of the $13/2^+$ isomeric state of ^{185}Hg is unambiguously established and γ-rays belonging to ^{185}Hg are known and located in the ^{185}Hg level scheme.

In this paper we report on the results obtained from three different experiments. The whole of the results have been used to determine a new or improved value of the energy location of the $13/2^+$ isomeric state relative to the ground state in ^{185}Hg, ^{189}Pb, ^{193}Po and ^{197}Rn.

To identify the γ-rays belonging to the ^{185}Hg nucleus and build a low-energy low-spin level scheme of ^{185}Hg, a new study of the β^+/EC decay of the ^{185}Tl nucleus has been performed, the experimental procedure and the results will be presented in sect. 2.

The decay of $^{185m+g}$Hg was studied by use of a Very Low-Energy Conversion Electron Detection, VLECED, setup [13]. The preliminary results of this experiment were reported in a conference only [14]. The high energy resolution electron spectrum recorded in this experiment has been carefully analysed using an internal calibration procedure, the experimental procedure will be briefly described and the results will be given in sect. 3. Moreover, by combining known α-decay properties of $^{185m+g}$Hg [15] and energy levels in ^{181}Pt [16,17], an independent value for the excitation energy of the ^{185}Hg isomer has been determined, the result will be also presented in sect. 3.

After a short description of the experiment performed to detect and identify the α particles emitted from the $^{189m+g}$Pb nucleus, the results that have served to determine the energy location of the isomeric state in ^{189}Pb, ^{193}Po and ^{197}Rn will be presented in sect. 4.

In sect. 5, the nuclear data and structures that are well established for the nuclei situated in the neighbourhood of ^{185}Hg and ^{189}Pb will be recalled very briefly, our results on the α-emitter chain starting with $^{197m+g}$Rn will be compared with those known on the α-emitter chains starting with $^{195m+g}$Rn and $^{199m+g}$Rn and then, the nuclear structure of the isomeric and ground states of the nuclei of these three chains will be discussed.

2 Low-energy levels of ^{185}Hg from β^+/EC decay of ^{185}Tl

2.1 Experimental procedure

The experiment was realized at the ISOLDE facility [18] at CERN. Radioactive atoms were produced by bombarding a thick uranium-carbide, UC_x, target with the 1.4 GeV protons delivered by the PS-Booster. The radioactive atoms released from the target effuse into a hot cavity where the Tl atoms are easily surface ionized. The ions were extracted using a high voltage of 60 kV and mass-separated by the General Purpose Separator, GPS. The mass-separated ion beam was then guided to a counting station, collected into a tape and, using the ISOLDE tape transport system, the obtained radioactive source was moved in front of three γ-ray detectors: one planar Ge(HP) X-ray detector with a 0.55 keV FWHM resolution at 80 keV and 0.9 keV at 356 keV, and two coaxial Ge(HP) detectors with about 70% relative efficiency and 2.5, 2.9 keV FWHM resolution at 1.33 MeV. Twenty milliseconds after a proton pulse hit the target, the radioactive ion beam was collected into the tape for a collecting time, $t_c = 2$ s, then, after the source transport time, $t_t = 1.5$ s, the γ-rays and X-rays from the source were counted for a measuring time, $t_m = 15.3$ s. This time cycle was repeated for 3 hours.

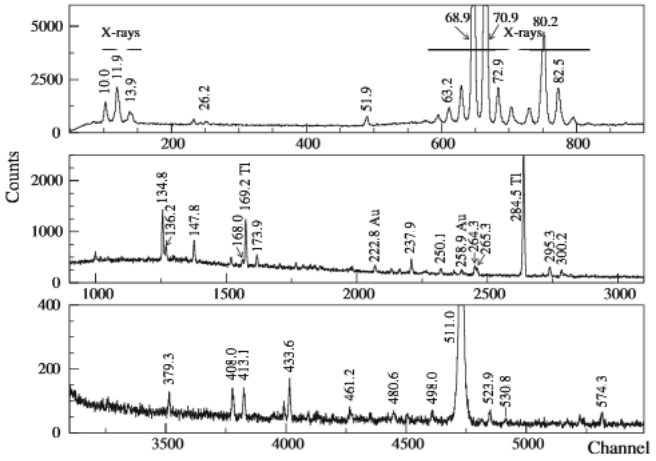

Fig. 1. Low-energy singles γ-ray spectrum obtained with the planar Ge(HP) X-ray detector. The γ-ray energies are given in keV.

The data were treated using a COMET-NARVAL acquisition system [19–21]. For each detected radiation the energy and absolute time were encoded by the COMET card. The NARVAL software served to associate energy and absolute time to create an event, to build on-line singles and coincidence control spectra and to send all information to be recorded on disk. From the recorded information, the coincidence events were built again off-line and sorted to get γ-γ-t and γ-X-t coincidence matrices.

2.2 Results

The singles γ-ray spectrum obtained with the X-ray detector is shown in fig. 1. The main γ-rays coincident with the X-rays are listed in table 1. The energy, intensity, main coincident γ-rays and location in the level scheme of the γ-rays belonging to the β^+/EC decay of the ^{185}Tl nucleus are given in table 2.

^{185}Tl is produced in both the $9/2^-$ isomeric and $1/2^+$ ground states that partly decay by α-particle emission.

Table 1. X-ray data for the ^{185r}Tl decay. X-ray intensities are given relatively to the ^{185m}Tl isomeric transition, 284.5 keV ($I_\gamma = 1000$). Parentheses mean uncertain coincidence relationship.

E(keV)[a]	I[b]		Main coincident γ-rays
10.0	43	XHg	
10.3	20	XTl	
11.5	16	XAu	
11.9	78	XHg	
12.3	37	XTl	
13.9	26	XHg	
14.3	21	XTl+XHg	
24.2	11	(XIn)	
63.2	19	XIr	
65.0	33	XPt+XIr	230[d]
67.0	80	XAu+XPt	223[e], 244[e], 259[e]
68.9	550	XHg+XAu	135,148, 163, 223[e], 238, 265, 300, 408, 434, 674
70.9	803	XHg+XTl	135,148, 163, 168, (174), 213, 238, 265, (293), 295, 300, (302), (336), 379, 408, 413, 431, 434, 461, (481), (498), (524), (531),(566), 630, (695), (804), 2099
72.9	80	XTl+XPb	169.2[f], 284.5[f]
73.4	8	XIr	
75.0	43	XPb+XPt+XIr	
77.9	41	XAu+XPt	190[e], (259)[e]
80.2[c]	273	XHg+XAu	135, (168), 174, 238, 265, 408, 434, 524
82.5	89	XTl+XHg	135
83.0	17	XTl+XHg	
84.8	21	XTl+XPb	

[a] $\Delta E_\square = 0.1$ keV for $I > 10$.
[b] $\Delta I_\square = 15\%$.
[c] A weak part of the intensity (not subtracted) could be due to transition in ^{181}Pt.
[d] Transition belonging partly to ^{181}Ir.
[e] Transition belonging to ^{185}Au.
[f] Isomeric transition in ^{185}Tl.

Their ^{185}Hg and ^{181}Au daughters and ^{185}Au, ^{185}Pt, ^{181}Au and ^{181}Pt granddaughters decay also by α and β^+/EC process. This results in complex γ-ray spectra in which γ-rays belonging to ^{181}Au, ^{181}Pt, ^{181}Ir and ^{177}Os are expected to be present in spite of the mass separation. These γ-rays have been identified from known data and/or their observation in coincidence with X-rays (see table 1).

The 169.2 keV ($I_\gamma = 128$) and 284.5 keV ($I_\gamma = 1000$) γ-rays observed with the strongest intensities (see fig. 1) are the isomeric transitions that de-excite the $9/2^-$ ^{185r}Tl isomeric state towards the $1/2^+$ ^{185r}Tl ground state. Their properties are in good agreement with those reported in the literature [22].

The 190.0 keV ($I_\gamma = 10$), 222.8 keV ($I_\gamma = 28$), 243.6 keV ($I_\gamma = 17$), 258.9 keV ($I_\gamma = 28$) γ-rays observed coincident with the Au X-rays belong to the β^+/EC decay of the $1/2^-$ ^{185}Hg ground state whereas no γ-ray of the β^+/EC decay of the $13/2^+$ ^{185}Hg isomeric state is observed (see table 1). This confirms that the $9/2^-$ ^{185r}Tl isomeric state decays by isomeric transitions and α particles only.

A 309.5 keV ($I_\gamma = 8$) γ-ray is also observed, it is a doublet composed of the 309.0 keV and 310.4 keV γ-rays that represents 16.6%, from ref. [23], of the ^{185}Au β^+/EC decay.

Two γ-rays with weak intensities: 94.0 keV ($I_\gamma \sim 7$) and 198.0 keV ($I_\gamma = 8$), correspond to transitions in ^{181}Pt. The α decay of the $1/2^-$ ^{185}Hg ground state does not feed the $7/2^-$ state located at 278.2 keV in the ^{181}Pt nucleus. Thus, the 198.0 keV γ-ray is only due to the ^{181}Au β^+/EC decay and represents 4.42%, from ref. [23], of this decay.

The 229.7 keV ($I_\gamma = 17$) γ line observed coincident with the Ir X-rays belongs, at least partly, to the β^+/EC decay of the ^{181}Pt nuclei produced from both the ^{181}Au β^+/EC decay and ^{185g}Hg α decay.

A partial level scheme, in three separate parts, of the ^{185}Hg nucleus (A, B and C shown in fig. 2) could be built from the data listed in table 2. Part A includes the 26 keV transition known to de-excite the first $3/2^-$ excited state towards the $1/2^-$ ^{185}Hg ground state [24]. It consists mainly of three couples of transitions having an energy difference of $\Delta E = 26.0(1)$ keV, namely: 147.8–173.9, 413.1–439.1 and 498–523.9 keV. A percentage of 21% of the total γ intensity ($I_{\gamma\mathrm{tot}} = 1800$) reported in table 2 has been located in this part of the level scheme. Part B consists of five transitions corresponding to 6% of

Table 2. γ-ray data for the β^+/EC decay of the ^{185}Tl ground state. γ-line intensities are given relatively to the ^{185m}Tl isomeric transition, 284.5 keV ($I_\gamma = 1000$). Parentheses mean uncertain coincidence relationship or tentative location.

E(keV)[a]	I[b]	Main coincident γ-rays	Location
26.2	8		$26.0 \rightarrow 0$
51.9	19	XHg	
134.8	81	XHg, 238, 434, (481, 520), 531	$134.8 + x \rightarrow x$
136.2	18	XHg	$136.2 + y \rightarrow y$
147.8	47	XHg, 265, (461)	$173.9 \rightarrow 26.0$
163.1	25	XHg	
168.0	24	136, 487	$304.1 + y \rightarrow 136.2 + y$
173.9	33	XHg	$173.9 \rightarrow 0$
212.8	22	(XHg)	
237.9	69	XHg, 135, 531, (661, 674, 739)	$372.7 + x \rightarrow 134.8 + x$
250.1[c]	18	(XHg)	
264.3	61	XHg, 484	
265.3	44	XHg, 148, (174)	$439.2 \rightarrow 173.9$
292.7	20	XHg, (168, 304)	$596.8 + y \rightarrow 304.1 + y$
295.3	87	XHg, 379	
300.2	52	XHg, (470, 520)	
301.7	25		
304.0	22	(293), 487	$304.1 + y \rightarrow y$
335.7[c]	14	(XHg), (434)	$903.8 + x \rightarrow 568.4 + x$
379.3	29	XHg	
408.0	79	XHg	
413.1	79	XHg	$(439.2 \rightarrow 26.0)$
431.1[c][d]	31	(XHg)	
433.6	103	XHg, 135, 336, (481, 520)	$568.4 + x \rightarrow 134.8 + x$
439.1	11		$(439.2 \rightarrow 0)$
453.1	15	566	
461.2	50	XHg	
465.6	12		$(1033.9 + x \rightarrow 568.4 + x)$
469.9	18	(300)	
478		(434)	$(1046.8 + x \rightarrow 568.4 + x)$
480.6[c][d]	34	XHg, 434, (498)	$1049.0 + x \rightarrow 568.4 + x$
483.7	7	264	
486.8	22	XHg, (168), 304	$790.9 + y \rightarrow 304.1 + y$
498.0	39	(624)	$(524.0 \rightarrow 26.0)$
519.8	30	XHg, (135, 300), 434	$1088.2 + x \rightarrow 568.4 + x$
523.9	65	XHg, 624	$524.0 \rightarrow 0$
530.8	26	(XHg), 135, 238	$903.8 + x \rightarrow 372.7 + x$
564.5	42	XHg	
566.1	21	453	
574.3	57	(XHg)	
624.4	17	XHg, 524	$1148.4 \rightarrow 524.0$
629.8	20	(148)	$(803.8 \rightarrow 173.9)$
661.2[c]	20	238	$1033.9 + x \rightarrow 372.7 + x$
674.1	15	238	$1046.8 + x \rightarrow 372.7 + x$
695.1	36	XHg	
738.5	8	238	$1111.2 + x \rightarrow 372.7 + x$
803.9	19		$(803.9 \rightarrow 0)$
1082.7	14	XHg, (461)	
1293.5	41		
1612.9	31	(413)	
1878.3	27		
2099.2	60		
2122.2	33		

[a] $\Delta E_\square = 0.1$ keV for $E_\square < 200$ keV, $I > 10$, 0.2 keV for $200 < E_\square < 1500$ keV, 0.3 keV for $E_\square > 1500$ keV.
[b] $\Delta I_\square = 15\%$.
[c] Intensities due to other decays have been subtracted.
[d] A weak part of the intensity (not subtracted) could be due to transition in ^{181}Pt.

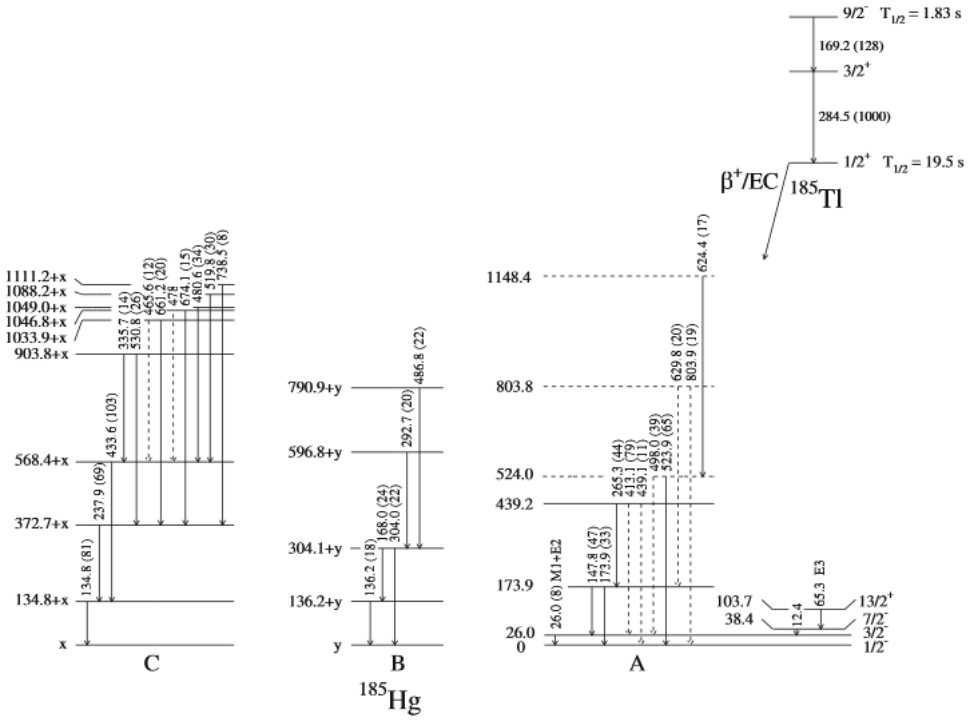

Fig. 2. Partial level scheme of ^{185}Hg obtained from the β^+/EC decay of the ^{185}Tl ground state. Parts B and C can be either on the $1/2^{\square}$ ground state or on top of the $3/2^{\square}$ state located at 26.0 keV. The decay of the ^{185m}Hg by isomeric transitions is shown on the right-hand side though it is not fed from the β^+/EC decay of ^{185}Tl (see text).

the total γ intensity. In part C, twelve transitions that represent 23% of the total γ intensity, have been placed. Though the $13/2^+$ isomeric state of ^{185}Hg is not fed from the β^+/EC decay of ^{185}Tl, its decay by isomeric transitions (obtained from ref. [24] and the results presented in sect. 3) is shown in fig. 2 on the right-hand side.

Only 26.2 and 51.9 keV γ-rays belonging to the ^{185}Tl β^+/EC decay have been observed in the γ spectrum with energy smaller than 130 keV. The multipolarity of the 51.9 keV transition is unknown, it may be $E1$ or more probably $M1$ or $M1+E2$, the total intensity of this transition may then vary from $I_{\rm tot} = 29$ for an $E1$, $I_{\rm tot} = 210$ for an $M1$, to $I_{\rm tot} = 2300$ for an $E2$ transition. Three couples of transitions with energy difference of 51.7(2) keV exist in table 2: 212.8–264.3, 250.1–301.7 and 379.3–431.1 keV but no coincidence relationship has allowed us to establish a partial level scheme including the 51.9 keV transition. The multipolarity of the 26.02(10) keV transition has been determined to be $M1 + (3.4(10)\%)E2$ (see next section), the total intensity of this transition is then rather high, $I_{\rm tot} = 1550(270)$. The ^{185}Tl ground state has spin and parity values, $I^\pi = 1/2^+$, it decays mainly to the $1/2^-$ and $3/2^-$ states of ^{185}Hg since no $1/2^+$ or $3/2^+$ state is expected to be located at low energy in this nucleus. Thus, the $3/2^-$ state located at 26.0 keV in ^{185}Hg may be fed directly by the ^{185}Tl β^+/EC decay, which is consistent with the large total intensity observed for the 26 keV transition. From part A of the level scheme the sum of the total intensities of the transitions arriving on the ground state is at least equal to 1678(289). In addition to that sum, the $1/2^-$ ground state of ^{185}Hg may also be fed directly by the ^{185}Tl β^+/EC decay. This means that transitions as the 295.3 keV that appears with high γ intensity in table 2 actually represent only a small percentage ($< 5\%$) of the ^{185}Tl β^+/EC decay. We note that, from the γ intensities measured, the 51.9 keV transition (except for a pure $E2$ multipolarity), part B and part C of the level scheme may be based either on the 26.0 keV state or on the ground state.

3 Low-energy transitions in ^{185}Au and ^{185}Hg from the $^{185m+g}$Hg decay

3.1 Experimental procedure

A measurement of the low-energy conversion electrons emitted from $^{185m+g}$Hg radioactive atoms were carried out using the VLECED system [13] that was installed at the ISOCELE facility [25]. Mercury atoms were produced by (p, xn) reactions on a molten gold target placed inside the ISOCELE mass separator ion source [26,27]. The 44 keV radioactive mercury beam extracted from the ion source was mass separated, decelerated and focused before being deposited on a transport tape as a very narrow spot. After the source was moved inside a 180° flat magnetic spectrograph, a high voltage of -10 kV was applied to it to accelerate the emitted electrons. Thus, the low-energy electrons could reach a photographic film and be detected.

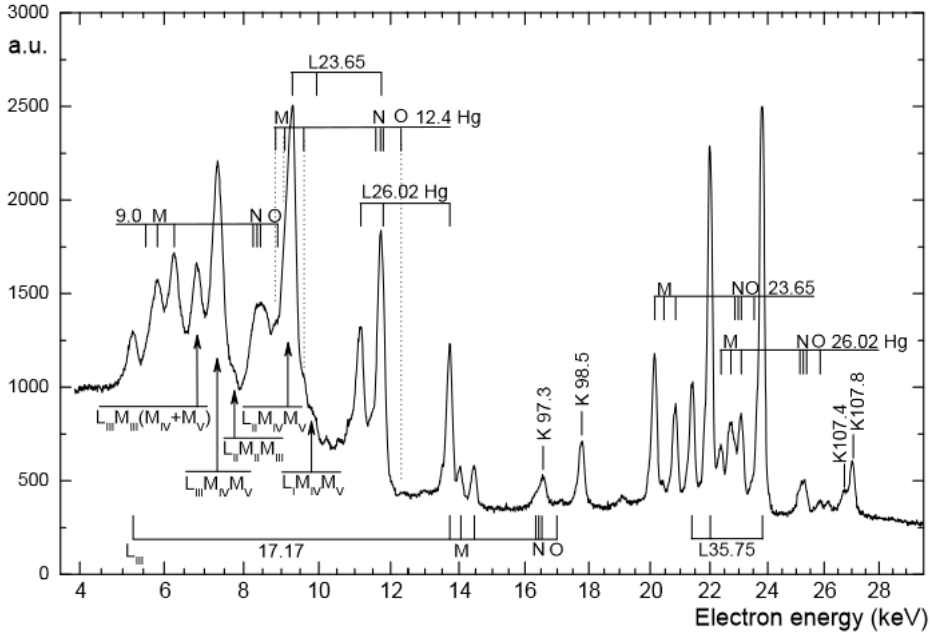

Fig. 3. Low-energy electron spectrum obtained for the $^{185m+g}$Hg decay using the flat magnetic spectrograph with $B = 5.10^{-3}$ T and $H.V. = -10$ kV. The transition energies are given in keV. The isomeric transitions in ^{185}Hg are marked with Hg. The electron lines that served to the internal energy calibration are indicated below the spectrum.

A high energy resolution was obtained even for the low-energy electrons thanks to the decelerating lens that preserved the quality of the beam focalisation and prevented too deep an implantation of the ions into the tape, for example, a resolution of 0.2 keV FWHM has been obtained at an electron energy of 14.4 keV. The slowed ion beam was deposited for a collecting time, $t_c = 30$ s, and then the accelerated electrons detected for a measuring time, $t_m = 30$ s, this time cycle was repeated until the total measuring time was 4 hours. The energies obtained with the flat magnetic spectrograph are expected to be very precisely measured (typically 0.05 keV) by the electron-line distance from notch positions used as geometric references. However, it has been shown that the high voltage applied to the electron source slightly modifies the electron trajectories in the spectrograph giving energy deviations for the electrons with energies smaller than 25 keV [28].

3.2 Results

The low-energy part of the electron spectrum obtained with a magnetic induction of 5×10^{-3} T is shown in fig. 3. The preliminary results obtained from this experiment were presented in a conference [14]. The $13/2^+$ isomeric state was then located at $E_{IS} = 103.8$ keV above the $1/2^-$ ground state of ^{185}Hg. In a second step, a careful analysis of the electron spectrum has been performed using an internal energy calibration procedure. The numerous LMM, LMN and LMO Auger electron lines of Au and Hg atoms have energies between 5 and 13 keV. They are observed in the part of interest of the electron spectrum. An Auger electron spectrum has been built from the calculated energies and intensities [29,30] of the 125, for Au, and 129, for Hg, main LMM, LMN and LMO Auger electron lines. The comparison of the calculated (80% Au + 20% Hg) Auger electron spectrum with the experimental ones has allowed us to unambiguously identify the 6.87 keV ($L_{III}M_{III}M_{IV} + L_{III}M_{III}M_V$), 7.35 keV ($L_{III}M_{IV}M_V$), 7.79 keV ($L_{II}M_{II}M_{III}$), 9.17 keV ($L_{II}M_{IV}M_V$) and 9.78 keV ($L_IM_{IV}M_V$) Au Auger electron lines. In addition to this, some transition energies belonging to ^{185}Au had been precisely determined using the same spectrograph but without high voltage applied to the source [24], conversion electron lines of two of them, also observed in the spectrum, served the internal energy calibration: namely L_{III}, M_{III} conversion electron lines of the 17.17(3) keV transition and L_I, L_{II}, L_{III} lines of the 35.75(5) keV transition. The electron energies, $E_{electron}$, electron intensities, I_e, transition multipolarities and total transition intensities, I_{total}, obtained for six low-energy transitions (four in Au and two in Hg) are listed in table 3. The energies of the Auger electrons and conversion electron lines that have served the internal calibration are indicated by superscript$^{(a)}$. The other electron energies have been obtained using the internal energy calibration procedure added to a shape analysis of the electron lines.

The L_{III} electron line of the 17.17 keV transition, M and N electron lines of the 9.0 keV and M_{III} and O electron lines of the 12.4 keV transition are observed for the first time in this experiment.

In the ^{185}Hg nucleus, the $13/2^+$ isomeric state decays partly to the $1/2^-$ ground state at least by a cascade of three transitions. Two of them were unambiguously identified as an $E3$ 65.3(1) keV and an $M1 + E2$ 26.1(1) keV isomeric transitions [24]. A slightly smaller energy, 26.02(10) keV, has been found for the second transition in our analysis of the electron spectrum (table 3).

Table 3. Low-energy conversion-electron data obtained from β^+/EC decay of $^{185m+g}$Hg and isomeric transitions of ^{185m}Hg.

Z	$E_{transition}$	$E_{electron}$		I_e, ref. [24]	I_e	Multipolarity	I_{total}
	keV		keV				
Au	Auger	$L_{III}M_{III}M_{IV+}L_{III}M_{III}M_V$	6.87[a]				
		$L_{III}M_{IV}M_V$	7.35[a]				
		$L_{II}M_{II}M_{III}$	7.79[a]				
		$L_{II}M_{IV}M_V$	9.17[a]				
		$L_IM_{IV}M_V$	9.78[a]				
Au	17.17(3)[a]	L_{III}	5.25[a]		195	$M1 + (0.5 < 0.7 < 1.3)\%E2$	760(180)
		M_I	13.74				
		M_{II}	14.02[b]	17	44.8		
		M_{III}	14.43[a]	18	43.5		
		M_{II}/M_{III}		0.944	1.03		
Au	35.75(5)[a]	L_I	21.40[a]	100	92.7	$M1 + 17(3)\%E2$	760(130)
		L_{II}	22.02[a]	230	233		
		L_{III}	23.83[a]	250	243		
		L_I/L_{II}		0.435	0.40(3)		
		L_I/L_{III}		0.40	0.38(3)		
		L_{II}/L_{III}		0.92	0.96(3)		
Au	9.00(13)	M_I	5.57[b]			$E2$	~ 1050
		M_{II}	5.82(8)		~ 360		
		M_{III}	6.28(8)		~ 460		
		N_I	8.24[b]				
		N_{II}	8.36[b]				
		N_{III}	8.46[b]				
Au	23.65(15)	L_I	9.30[b]		407[d]	$M2$	940(120)
		L_{II}	9.92[b]		20[d]		
		L_{III}	11.71(10)		233[d]		
		M_I	20.22[b]	**110**	**110**		
		M_{II}	20.50[b]	13	~ 17		
		M_{III}	20.91[b]	78	77.7		
		N_I	22.89(5)				
		N_{III}	23.17(10)				
Hg	12.40(20)	M_I	8.84[b]		3.2(6)[d]	$E2$	627(113)
		M_{II}	9.12[b]		179(33)[d]		
		M_{III}	9.55(15)		231(42)[d]		
		N_{II}	11.72[b]		45(8)[d]		
		N_{III}	11.82[b]		57(11)[d]		
Hg	26.02(10)	L_I	11.18[b]	[16–18.8[c]]	145(20)	$M1 + 3.4(10)\%E2$	627(113)
		L_{II}	11.81[b]	[12.3–20.9[c]]	120[d]		
		L_{III}	13.74(7)	[8.6–22.1[c]]	111(39)		
		L_I/L_{III}		[0.72–2.19]	1.31		
		M_I	22.46[b]	5.5[c]	44.7		
		M_{II}	22.74[b]	4.4[c]			
		M_{III}	23.17[b]	5.4[c]			
		$M_{II+}M_{III}$			91.3		
		$M_I/(M_{II+}M_{III})$		0.56	0.49(10)		
		$N_I + N_{II} + N_{III}$	25.3[b]		30.3		
		$L_I/(N_I + N_{II} + N_{III})$			4.8(7)		
		$L_{III}/(N_I + N_{II} + N_{III})$			3.7(13)		
		$M_I/(N_I + N_{II} + N_{III})$			1.50(15)		
		$(M_{II} + M_{III})/(N_I + N_{II} + N_{III})$			3.0(3)		

[a] Used for energy calibration.
[b] From transition and binding energies.
[c] Intensity per 100 decays of ^{185m}Hg.
[d] Intensity estimated from multipolarity, conversion coefficients and measured I_e or I_{total} for the $E2$ 12.4 keV transition.

Table 4. Data from $^{185m+g}$Hg α-decay measurements, from [15,23,31–34]. The q value reported in the last column corresponds to the nucleus-recoil energy, E_r, added to the α-particle kinetic energy, E_α, ($q = E_r + E_\alpha$). For α transition between ground states the q value corresponds to the usual Q_α value.

	I^π	E_α (keV) [31]	E_α (keV) [15]	E_α (keV) [32]	Coincident γ-rays [15]	E_α (keV) [33,34]	I_α (%) [23,33,34]	HF [33]	q (keV)
^{185g}Hg	$1/2^{\square}$	5652(15)	5652	5652		5653(5)	5.8	1.15	5778(5)
		5575(15)	5560	5575	79, 94	5569(5)	0.24	10.2	5692(5)
				5560					5683
^{185m}Hg	$13/2^+$		5430		161	5430	≤ 0.006	≥ 45	5550
			5410		161	5408(10)	0.006	32	5528(10)
		5375(15)	5365		61, 106, 118, 161	5372(8)	0.024	6	5491(8)

The third isomeric transition must be then an $E2$ transition with energy smaller than 16 keV and the same total intensity as that of the 26.1 keV isomeric transition [24]. A 9.55(15) keV electron line is observed between the L_I ($E_e = 9.30(15)$ keV) electron line of the 23.65 keV and the 9.78 keV ($L_I M_{IV} M_V$) Auger line. If this line was an L_{III} line corresponding to a 21.83 keV transition, the 7.62 keV L_{II} line should be observed as a tail on the right of the 7.35 keV $L_{III}M_{IV}M_V$ Auger line, but it is not. Furthermore, the 18.55 keV M_{II} and 18.98 keV M_{III} lines of this 21.83 keV that would have respectively 8.5% and 10% of the total intensity of the transition, should be also observed, with a larger intensity than that of the M_I line of the 26.02 transition that has only 6.3% of the total intensity of the transition, but neither of these two electron lines is observed. Therefore, the 9.55 keV electron line is an M_{III} electron line, the M_{II}, N_{II} and N_{III} lines are then forming doublets with the 9.17 keV ($L_{II}M_{IV}M_V$) Auger line, with the L_{III} ($E_e = 11.71(10)$ keV) of the 23.65 keV transition and with the L_{II} ($E_e = 11.81(10)$ keV) of the 26.02 keV transition, respectively. Unfortunately, given the complexity of the electron spectrum around 9.3 keV, the intensities of the M electron lines could not be determined and the intensities reported in column 6 of table 3 have been estimated from the total intensity of the 26.02 keV transition using the $E2$ internal conversion coefficients. Thus, the careful analysis of the electron spectrum indicates that a 12.40(20) keV $E2$ transition exists in the decay of the $13/2^+$ isomeric state of ^{185}Hg that is then located at $E_{IS} = 103.72(40)$ keV.

We could imagine that the isomeric cascade consists of four transitions instead of three: two $M1$ transitions instead of the 12.4 keV $E2$ transition. The 9.55 keV electron line could be then the M_I lines of one 13.1 keV $M1$ transition, the other one would have a smaller energy, which would locate the isomeric state at $E_{IS} < 117.5$ keV. The existence of a fourth transition in the isomeric cascade cannot be completely excluded experimentally. However, this hypothesis is highly improbable since no $5/2^-$ state is expected to be located at so low energy in ^{185}Hg from systematic energy studies performed for known states in $Z = 76$, 78 and 80 and $N = 105$ nucleus series (see fig. 10 in sect. 4).

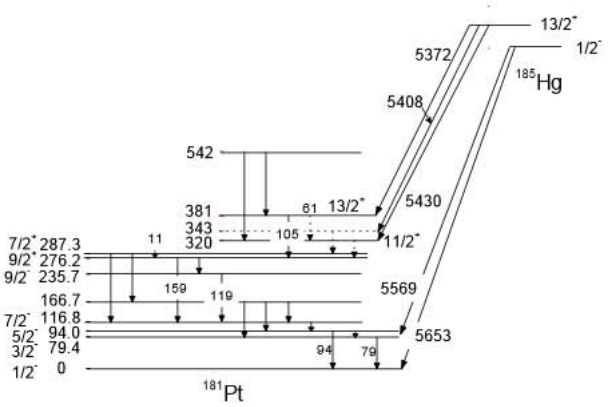

Fig. 4. Levels of the ^{181}Pt nucleus fed directly or indirectly from the $^{185m+g}$Hg α decay. The de-excitations of the 542 keV level that allow the energy location of the 381 keV level relatively to the 320 keV level, are also shown. Information is taken from refs. [15–17,23,33,34], energies of the levels and transitions observed coincident with the α lines are given in keV.

It is worth noting that the conversion electron lines of the 51.9 keV transition detected in the ^{185}Tl β^+/EC decay (sect. 2) are not observed in the electron spectrum, which proves that this 51.9 keV transition does not participate to the de-excitation of the $13/2^+$ isomeric state to the $1/2^-$ ground state of ^{185}Hg.

The α decay of $^{185m+g}$Hg was studied extensively [15, 31,32] but at that time no information on the ^{181}Pt level scheme was available. Five α lines were observed: two from the $1/2^-$ ground state and three from the $13/2^+$ isomeric state of ^{185}Hg. Some of these α lines were observed to be coincident with γ-rays [15]. The results from the α-decay studies are summarized in table 4. Since then, excited states of ^{181}Pt have been established from radioactivity [17] and (HI, $xn\gamma$) reaction [16] studies. Almost all of the γ-rays observed in coincidence with the α particles are placed in the ^{181}Pt level scheme. The ^{181}Pt levels of interest for the subject are shown in fig. 4.

The 79.4 and 94.0 keV γ-rays are observed coincident with the 5569 keV α particles and the 79.4 keV γ line appears clearly with a higher intensity than the 94.0 keV γ line in the α-γ coincidence spectrum shown in ref. [15]. For the de-excitation of the 94.0 keV state of ^{181}Pt, the γ-ray intensity of the 79.4 keV transition can be estimated to be 56(10)% of that of the 94.0 keV transition from the data reported in ref. [17], which means that the 5569 keV α line is a doublet. One of the α transitions feeds the 79.4 keV state and the other one the 94.0 keV state of the ^{181}Pt nucleus as previously suggested in ref. [32].

Two positive-parity states, $9/2^+$ and $(7/2^+)$, have been located, respectively, at 276.2 keV and 287.3 keV in ^{181}Pt [17]. The $11/2^+$ and $13/2^+$ states of the rotational band based on the $9/2^+$ state have been established at 320 and 381 keV, respectively, and the 105 keV $13/2^+ \rightarrow 9/2^+$ transition has been observed [16]. This 105 keV transition corresponds to the 106 keV γ-ray seen coincident with the 5372 keV α particles. The $13/2^+$ state is located at 61 keV above the $11/2^+$ one, the 61 keV γ-ray observed coincident with the 5372 keV α line is then very likely the $13/2^+ \rightarrow 11/2^+\gamma$ transition. This 61 keV γ-ray was too low in energy to be detected in the in-beam experiment. The 161 and 118 keV γ-rays also coincident with the 5372 keV α line are the 159.4 and 118.9 keV γ-rays that de-excite the $9/2^+$ state at 276.2 keV and the $9/2^-$ state at 235.7 keV (see fig. 4). All of these data indicate very clearly that the 5372 keV α decay feeds the $13/2^+$ state located at 381 keV in ^{181}Pt. The 5430 keV α decay probably feeds the $11/2^+$ state at 320 keV since the energy difference of the q values corresponding to the 5430 and 5372 keV α particles is 59(10) keV in perfect agreement with the 61 keV energy difference between the $11/2^+$ and $13/2^+$ states (see fig. 4 and table 4).

The 5408 keV α decay feeds very likely an $11/2^+$ or $13/2^+$ state belonging to the rotational band, not observed up to now, based on the $7/2^+$ state located at 287.3 keV in the ^{181}Pt nucleus.

These α-decay results of the $^{185m+g}$Hg nucleus indicate that the isomeric state is located at 94(13) keV above the ^{185}Hg ground state. This value is in agreement within the error bars with the electron determination $E_{IS} = 103.7(4)$ keV.

On the other hand, the energy of this isomeric state was determined to be $E_{IS} = 120(5)$ keV from mass measurement performed by use of the Penning-trap mass spectrometer ISOLTRAP [35]. This value differs by $\Delta E_{IS} = 16$ keV, representing more than 3 standard deviations, from that determined from our conversion electron measurement. This E_{IS} value would imply an energy of 28.7(50) keV for the $E2$ transition of the cascade of which we should have observed the L_{II} ($E_e = 14.5(50)$ keV), L_{III} ($E_e = 16.4(50)$ keV), M_{II} ($E_e = 25.4(50)$ keV), and M_{III} ($E_e = 25.9(50)$ keV) internal conversion electron lines since their intensities would be 35%, 39%, 9% and 10% of the total intensity of the transition respectively whereas, for the 26.02 keV transition, the intensity of its L_I electron line is 27% of its total intensity. In fig. 3, we can see that all electron lines observed with an energy higher than 9.8 keV are properly identified, which means that the existence of an $E2$ 28.7(50) keV transition with the same intensity as the 26.02 keV has to be ruled out.

It is worth, however, noting that Schwarz **et al.** [35] mentioned the possible existence of an unexpected systematic error and added quadratically an error of 20 keV before performing mass evaluation. If such a systematic error played a role on the determination of the isomeric state energy in ^{185}Hg then, the energy $E_{IS} = 120(21)$ deduced from mass measurement would be in reasonable agreement with both energies $E_{IS} = 94(13)$ keV and $E_{IS} = 103.7(4)$ keV obtained from the $^{185m+g}$Hg α decay and our electron measurement, respectively.

We shall adopt $E_{IS} = 103.7(4)$ keV as energy of the isomeric state of the ^{185}Hg nucleus in the next sections.

4 Study of the α decay of $^{189m+g}$Pb

4.1 Experimental procedure

Lead radioactive atoms were produced in the same way as the thallium atoms (see sect. 2.1). The Tl atoms are surface ionized in the hot cavity whereas the Pb atoms are selectively photo-ionized in a three-step resonant process using the Resonance Ionization Laser Ion Source, RILIS [36,37], of the ISOLDE facility. To ionize the lead atoms the laser beam wave length was: for the first excitation step, $\lambda = 283.3$ nm, for the second excitation step, $\lambda = 600.2$ nm and for the ionization step, $\lambda = 511$ and 578 nm [11,12]. The lead ions extracted by a 60 kV high voltage were mass-separated and then guided to a counting station. The ion beam was collected into the tape of a tape transport system with precise and reliable movements [38]. Then the source was moved in front of three detectors: one implanted Si α detector (100 mm^2 area and 100 μm thickness) with 14 keV FWHM resolution at 5.7 MeV and two coaxial Ge(HP) γ detectors (60% relative efficiency, 3.6 keV FWHM resolution at 1.33 MeV and 70% relative efficiency, 4.3 keV FWHM resolution at 1.33 MeV).

Two measurements have been realized. For the first one the laser beam frequency of the first excitation step was set at 17643.20 cm^{-1} (before frequency doubling) to ionize with a good efficiency both the atoms with ^{189m}Pb and ^{189g}Pb nuclei. The ion beam was collected for $t_c = 300$ ms immediately after the proton pulse and measured for $t_m = 52$ s after the source transport time, $t_t = 315$ ms. Both α-γ and γ-γ coincidence measurements were performed for 10 hours. For the second one the laser beam was used in a narrow band mode and a frequency scan of 28 steps of $\delta\nu = 0.02$ cm^{-1} has been realized to obtain hyperfine spectra by measuring the α-line and γ-line intensity changes against the frequency value. For every frequency step one source was collected for $t_c = 2.5$ s immediately after the proton pulse and measured for $t_m = 54$ s after the tape movement. This measurement has been repeated four times: two while the laser frequency was increased and two while it was decreased.

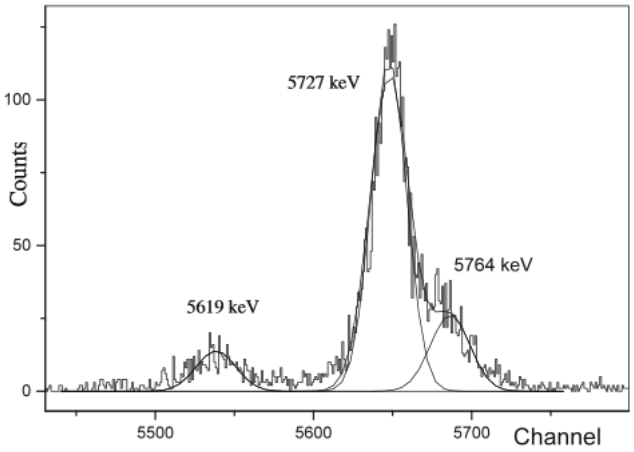

Fig. 5. α-γ matrix projection on the α axis, energies are given in keV.

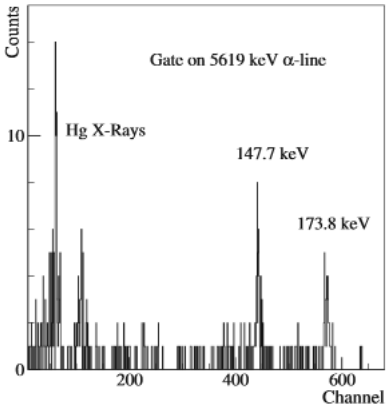

Fig. 6. γ spectrum for gate on the 5619 keV α line, energies are given in keV.

The data are treated using the COMET-NARVAL acquisition system (see sect. 2.1).

The experimental procedure has been described with many more details in refs. [12,39].

4.2 Results

The α-γ matrix projection on the α axis and the γ spectrum observed in coincidence with the 5619 keV α particles are shown in figs. 5 and 6. Three α decays of the ^{189}Pb nucleus were observed with energies of 5619, 5727 and 5764 keV. Only a 5730 keV α decay was already known [40]. The 5619 and 5764 keV α decays were therefore observed for the first time. We have to note that in fig. 5 the 5619 keV α line seen in the spectrum is mainly due to α-γ true coincidences and represents around 4% of the detected 5619 keV α particles whereas the 5727 keV and 5764 keV α lines are only due to α-γ random coincidences and represent only around 0.7% of the detected α particles. The 147.7 and 173.8 keV γ-rays appear to be coincident with the 5619 keV α particles. No γ-ray has been seen coincident with the 5727 and 5764 keV α particles. These two γ-rays were also observed in our ^{185}Tl

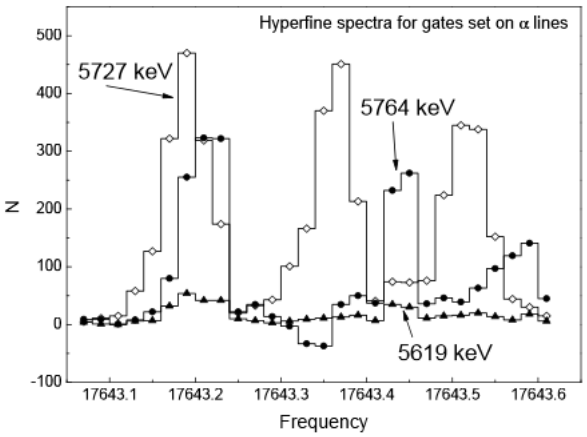

Fig. 7. Hyperfine spectra for gates set on the 5727, 5764 and 5619 keV α lines, N is the α-line intensity. Frequency values in cm^{-1} correspond to the laser beam of the first excitation step before doubling.

β^+/EC decay study and they de-excite the 173.9 keV level of ^{185}Hg (see sect. 2.2 and part A of fig. 2). Thus the α-γ coincidence results indicate clearly that the 5619 keV α decay feeds directly the 173.9 keV level of ^{185}Hg. The energy difference of the q values corresponding to the 5764 and 5619 keV α decays, $\Delta q = 149(4)$ keV, is consistent with the 5764 keV α decay feeding the 26.0 keV level of ^{185}Hg.

The hyperfine spectra corresponding to the 13/2 and 3/2 states of the neutron-deficient Pb nuclei are very different and well identified [12,39]. The intensity variations of the α lines with the laser beam frequency have provided the hyperfine spectra shown in fig. 7. The hyperfine spectrum obtained for a gate set on the 5727 keV α line indicates unambiguously that these α particles come from the 13/2 state of ^{189}Pb whereas the hyperfine spectra obtained for the two other α lines indicate that both the 5764 and 5619 keV α particles are emitted by the 3/2 state of ^{189}Pb.

The α results are given in table 5 and the α-decay scheme of $^{189m+g}$Pb is shown in fig. 8.

These results allow us to locate the $13/2^+$ at 40(4) keV above the $3/2^-$ ground state of the ^{189}Pb nucleus. The intensity of the direct β^+/EC decay of the $3/2^-$ ^{189}Pb ground state towards the $1/2^+$ ^{189}Tl ground state being unknown, only limits could be estimated for the absolute intensities, I, and hindrance factors (determined as described in ref. [42]), HF, of the α decays of the $3/2^-$ ground state of ^{189}Pb (see table 5). It is worth noting that the systematic error mainly due to calibration uncertainty, changes in the same way the E_α values since they differ of only some percents, which results to an error of some percents of the systematic error on the Δq difference (i.e. around 0.1 keV for ^{185}Hg). The systematic error plays a role on the mass determination accuracy, Q_α value, only.

It is clear that the determination of the energy location of an isomeric state can serve to estimate the energy location of the isomeric state of its parent provided the energies of the α particles emitted by the two parent iso-

Table 5. α-particle data for α decay of the $^{189m+g}$Pb isomers. Values in first and second parentheses are statistical and systematic errors on the α energies, respectively. HF: Hindrance factors are determined using the way described in ref. [42], $q = E_r + E_\alpha$, the q value corresponds to the usual Q_α value for the α transition between the ground states.

	I^π	$T_{1/2}$ (s) [39]	E_α (keV) [40]	E_α (keV)	Coincident γ-rays	I_α	I_α (%)	HF	q(keV)
^{189}Pb	$3/2^{\square}$	39(8)		5764(3)(5)		23	≤ 0.36	≥ 4	5889
				5619(2)(5)	147.7, 173.8	2.5	≤ 0.04	≥ 8	5740
	$13/2^+$	50(3)	5730(10)	5727(2)(5)		100	$\approx 0.4^{(a)}$	≈ 3.4	5851

(a) From [41].

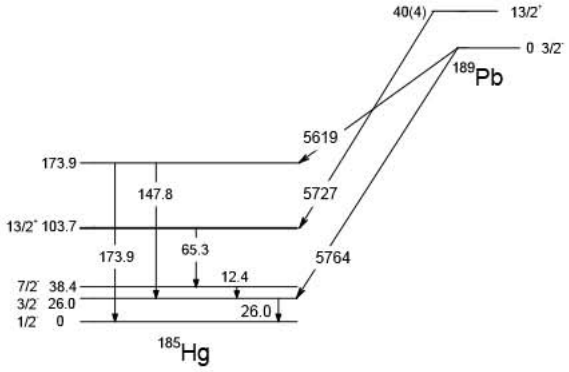

Fig. 8. α-decay schemes of the $^{189m+g}$Pb isomers. Energies are given in keV.

mers are known and located in a α-decay scheme. The α-decay data (spin and parity values of the initial and final states, I_i^π, I_f^π, half-life of the initial state, $T_{1/2}$, energy of the α particles, E_α, α-transition intensity, I_α, q value ($E_r + E_\alpha$), hindrance factor, HF) known for the α-emitter chains starting with the $^{195m+g}$Rn, $^{197m+g}$Rn, $^{199m+g}$Rn nuclei have been listed in table 6. The partial α-decay schemes of the nuclei of these three α-emitter chains are shown in fig. 9. Only the main α decays are represented. The energies of the α particles from $^{193m+g}$Po (table 6) added to the energy location at 40(4) keV of the $13/2^+$ isomeric state of ^{189}Pb determined in the present work have allowed us to locate the $13/2^+$ isomeric state at 95(7) keV above the $3/2^-$ ground state of the ^{193}Po nucleus. In the same way, $13/2^+$ isomeric states have been located at 194(12) keV and 63(29) keV above the $3/2^-$ ground states of the ^{197}Rn and ^{187}Hg nuclei, respectively. From mass measurement performed using the ISOLTRAP setup the isomeric state of ^{187}Hg has been located at 54(7) keV [35]. This more precise value is in agreement within the error bars with our value and will be adopted later on (see fig. 9). No α particle from the $13/2^+$ isomeric state of ^{191}Pb has been observed up to now, which prevents us from estimating the energy location of the $13/2^+$ isomeric states of the ^{191}Pb, ^{195}Po and ^{199}Rn nuclei (noted as y, $y + 95$ and $y + 168$, respectively, in fig. 9).

As for the third chain, several experiments have shown that there is no $13/2^+$ isomeric state with half-life in the order of 1s in the ^{183}Hg nucleus: i) all the observed α decays emitted by this nucleus come from the $1/2^-$ ground state, ii) no internal-conversion electron line due to isomeric transitions in ^{183}Hg has been observed [65], iii) whereas the β^+/EC decay of the $13/2^+$ isomeric state of ^{185}Hg feeds states with I value up to 17/2 in ^{185}Au [24, 66], the β^+/EC decay of ^{183}Hg feeds only states with $I < 13/2$ in ^{183}Au since no γ-ray observed in the in-beam study has been seen in the β^+/EC decay study [65, 67]. Thus, the $13/2^+$ observed as a isomeric state in the in-beam study of ^{183}Hg [68,69] is very likely located at a higher energy than either a $9/2^-$ or a $9/2^+$ state.

The 9/2 states expected to be located at low energy in ^{183}Hg can be deduced from the energy evolution of the level unambiguously identified in the isotones $N = 103$ and $N = 105$, see fig. 10. In the rotational bands built on the $1/2^-$ ground states of the ^{179,181,183}Pt and ^{183}Hg nuclei the $3/2^-$ states are located at less than 20 keV under the $5/2^-$ states. This property indicates unambiguously that the $1/2^-$ ground states are the $1/2^-[521]$ Nilsson states corresponding to a prolate nuclear shape [69, 70]. Shi **et al.** [69] and Lane **et al.** [68] have observed the $1/2^-[521]$ rotational band in ^{183}Hg from in-beam experiments. Their results differ only for the two first $3/2^- \rightarrow 1/2^-$ and $5/2^- \rightarrow 1/2^-$ transitions. Shi **et al.** [69] observed an 88.9 keV γ-ray coincident with the γ lines of the favoured $1/2^-[521]$ band and an 86.5 keV γ-ray coincident with the γ lines of the disfavoured $1/2^-[521]$ band. Therefore, they have attributed the 88.9 keV and 86.5 keV γ-rays to the $5/2^- \rightarrow 1/2^-$ and $3/2^- \rightarrow 1/2^-$ transitions, respectively. Lane **et al.** [68] saw a 66.8 keV and an 87 keV γ-rays coincident with a γ line of the favoured $1/2^-[521]$ band and determined an $M1 + E2$ multipolarity for the 66.8 keV transition. Therefore, they have tentatively attributed the 66.8 keV and 87 keV γ-rays to the $3/2^- \rightarrow 1/2^-$ and $5/2^- \rightarrow 1/2^-$ transitions, respectively. Thus, the $9/2$ $1/2^-[521]$ has been located at 288 keV [69] and at 286 keV [68] in ^{183}Hg, in fig. 10 we have adopted the data from [69] for the $1/2^-[521]$ band since three interband transitions supported their results.

Table 6. α-decay data: spin and parity values of the initial and final states, I_i^π, I_f^π, half-life of the initial state, $T_{1/2}$, energy of the α particles, E_α, α-transition intensity, I_α, $q(E_r + E_\alpha)$ value and Hindrance factor, HF, known for the α-emitter chains starting with the $^{195m+g}$Rn, $^{197m+g}$Rn, $^{199m+g}$Rn nuclei. For α transition between ground states the q value corresponds to the usual Q_α value.

	A	I_i^π	I_f^π	$T_{1/2}$(s)	E_α (keV)	I_α (%)	q(keV)	HF		Other references
Rn	199	$(3/2^\square)$	$(3/2^\square)$	0.59(3)	6989(6)	94	7132	0.98	[43]	[44–47]
	199	$(13/2^+)$	$(13/2^+)$	0.31(2)	7060(6)	97	7205	0.9		
	197	$(3/2^\square)$	$(3/2^\square)$	0.066(16)	7260(7)	100	7410	1.5	[48]	[49]
	197	$(13/2^+)$	$(13/2^+)$	0.021(5)	7357(6)	100	7509	1.0		
	195	$(3/2^\square)$	$(3/2^\square)$	0.006(3)	7536(11)	99.75	7694	2.4	[50]	[51]
	195	$(13/2^+)$	$(13/2^+)$	0.005(3)	7555(11)	99.8	7713	2.3		
Po	195	$(3/2^\square)$	$3/2^\square$	4.64(9)	6606(5)	99.56	6744	1.6	[52]	[47,50,53]
	195		$(5/2^\square)$		6399(10)	0.054	6533	465		
	195		$(3/2^\square)$		6027(5)	0.34	6153	2.0		
	195				5985(10)	0.036	6110	12		
	195	$(13/2^+)$	$13/2^+$	1.92(2)	6699(5)	99.83	6839	1.6		
	195		$13/2^+$		6047(5)	0.17	6174	2.1		
	193	$(3/2^\square)$	$3/2^\square$	0.42(4)	6948(4)	99.3	7095	2.5	[54]	[47,49,53,55,56]
	193		$3/2^\square$		6420(20)	0.7	6556	3.7		
	193	$(13/2^+)$	$13/2^+$	0.24(1)	7002(4)	99	7150	2.1		
	193		$13/2^+$		6375(15)	0.8	6510	1.2		
	191	$(3/2^\square)$	$13/2^+$	0.022(1)	7336(15)	14.9	7493	21	[57]	[58–60]
	191		$3/2^\square$		7334(5)	76	7491	4		
	191		$(3/2^\square)$		6966(10)	7.9	7115	2.3		
	191	$(13/2^+)$	$13/2^+$	0.093(3)	7376(5)	45.7	7534	70		
	191				6909(15)	3.7	7057	26		
	191		$(13/2^+)$		6888(5)	36	7035	2.2		
	191				6815(15)	9.6	6961	4.5		
	191				6790(15)	0.5	6935	76		
Pb	191	$3/2^\square$	$3/2^\square$	79.8(5)	5310(10)	0.013	5424	0.46	[52]	[41,57,61]
	189	$3/2^\square$	$3/2^\square$	39(8)	5764(3)(5)	≤ 0.36	5889	≥ 4		
	189				5619(2)(5)	≤ 0.04	5740	≥ 8		–
	189	$13/2^+$	$13/2^+$	51(3)	5727(2)(5)	0.4[(a)]	5851	3.4		
	187	$3/2^\square$	$(1/2, 3/2, 5/2)^\square$	15.2(3)	6194(10)	4.2	6329	9.1	[62]	[61,63]
	187		$(3/2^\square)$		5993(10)	2.8	6124	2.2		
	187	$13/2^+$	13/2+	18.3(3)	6077(7)	12	6210	1.4		
Hg	187	$3/2^\square$	3/2 1/2$^\square$ [521]	114(18)	5035(20)	$> 2.5E-04$	5145	< 50	[23]	[31]
	187	$13/2^+$	13/2 9/2$^+$[624]	144(18)	4870(20)	$> 1.2E-04$	4976	< 14		
	185	1/2 1/2$^\square$ [521]	1/2 1/2$^\square$ [521]	49.1(10)	5653(5)	5.8	5778	1.15	[33]	[15,23,31,32]
	185		3/2 et 5/2 1/2$^\square$ [521]		5569(5)	0.24	5692	10.2		
	185	$13/2^+$	11/2 9/2$^+$[624]		5430	≤ 0.006	5550	≥ 45		
	185		(11/2,13/2) 7/2$^+$[633]	21.6(15)	5408(10)	0.006	5528	32		
	185		13/2 9/2$^+$[624]		5372(8)	0.024	5491	6		
	183	1/2 1/2$^\square$ [521]	1/2 1/2$^\square$ [521]	9.4(7)	5904(5)	11	6036	1.8	[64]	[32]
	183		3/2 1/2$^\square$ [521]		5834(10)	0.61	5964	15		
	183		5/2 1/2$^\square$ [521]		5819(10)	0.43	5949	18		
	183		7/2 1/2$^\square$ [521]		5669(10)	0.035	5796	48		

[(a)] From ref. [41].

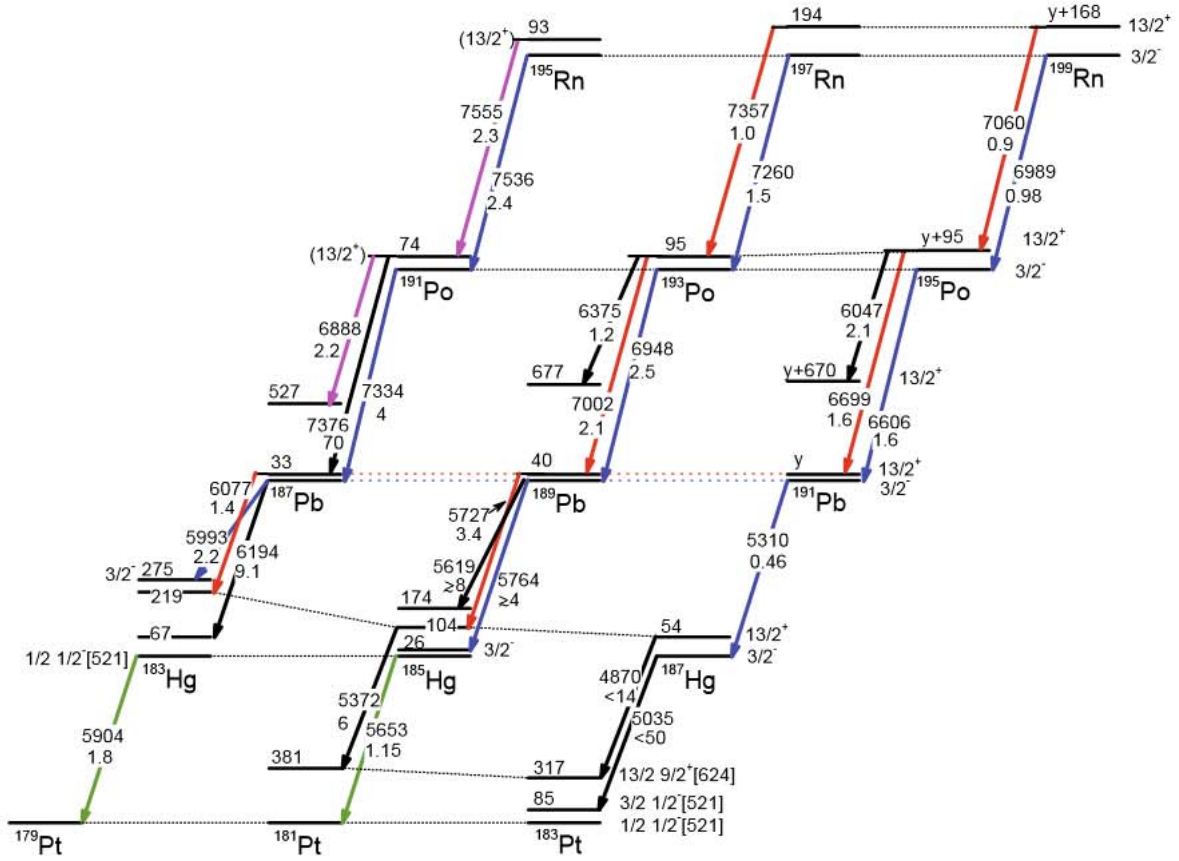

Fig. 9. Partial decay schemes of the nuclei of the α-emitter chains starting with the $^{195m+g}$Rn, $^{197m+g}$Rn, $^{199m+g}$Rn nuclei. Energies are given in keV and HF values are indicated below the α energies.

A $9/2^+[624]$ state due to the strong coupling of the $i_{13/2}$ neutron with the core is also expected lying at low energy in ^{183,185}Hg. However, this $9/2^+$ state is probably located slightly above the $13/2^+$ level from the results obtained on ^{183,185}Hg using in-beam experiments [68,69,71]. The properties of the rotational bands built on the $7/2^-$ levels lying at low energy in ^{179,181}Os [72–74], ^{181,183}Pt [16, 17,75,76] and ^{183,185}Hg nuclei ([14,24,68,69,71] and this work) indicate very clearly that these $7/2^-$ levels are the $7/2^-[514]$ Nilsson states. In ^{183}Hg the $7/2^-[514]$ state has not been placed in the level scheme but from fig. 10 we can estimate that it should be located at 120(10) keV. The $9/2 \rightarrow 7/2$ intra-band transition energy is 105 keV, which gives an energy location of the $9/2\ 7/2^-[514]$ state around 225 keV. This latter state that is then the 9/2 level located at the lowest energy is indeed the best candidate to serve to de-excite the $13/2^+$ isomeric state. Thus, in ^{183}Hg the $13/2^+$ state is expected to be located at a higher energy than 225 keV.

This $13/2^+$ isomeric state in ^{183}Hg is very probably fed directly by the unhindered (HF = 1.4) 6077 keV α transition coming from the $13/2^+$ state of ^{187}Pb. From a α-decay study of ^{191}Po Andreyev **et al.** [60] have located the $3/2^-$ state in ^{187}Pb at $E_{IS} = 2(15)$ keV above the $13/2^+$ state that is then the probable ground state of ^{187}Pb. From this $E_{IS} = 2(15)$ keV value in ^{187}Pb we can

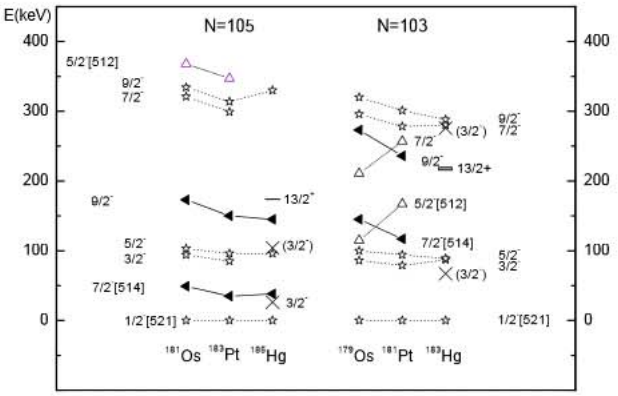

Fig. 10. Systematics of the state energies known in the $N = 105$ and $N = 103$ isotones: stars for the $1/2^\square$ [521] band states, open triangles for the $5/2^\square$ [512] band states, full triangles for the $7/2^\square$ [514] band states and × for $3/2^\square$ and $(3/2^\square)$ states. $13/2^+$ isomeric state is shown as a horizontal line in ^{185}Hg and as a rectangle (because of the large uncertainty $E_{IS} = 219(18)$ keV) in ^{183}Hg.

deduce an energy location of the $13/2^+$ state in ^{183}Hg at $E_{IS} = 184(19)$ keV.

Besides, mass measurements performed using ISOLTRAP have allowed Weber **et al.** [77] to locate

Table 7. Known β, I and μ values of the isomeric and ground states of the Pb, Hg and Pt nuclei next to the ^{185}Hg and ^{189}Pb nuclei and of the 3/2 1/2$^{\square}$ [510] state of ^{183}Os.

	A	I_{gs}	μ (μ_N)	$\langle\beta^2\rangle^{1/2}$	I_{ls}	μ (μ_N)	$\langle\beta^2\rangle^{1/2}$	refs.
Pb	187	$3/2^{\square}$	-1.126	< 0.1	$13/2^+$	-1.21	< 0.1	[12]
	189	$3/2^{\square}$	-1.081	< 0.1	$13/2^+$	-1.19	< 0.1	[12]
	191	$3/2^{\square}$			$13/2^+$	-1.176	0.065	[78]
Hg	183	$1/2^{\square}$	0.524	0.27				[1]
	185	$1/2^{\square}$	0.509	0.25	$13/2^+$	-1.017	0.15	[1]
	187	$3/2^{\square}$	-0.594	0.15	$13/2^+$	-1.044	0.14	[1]
Pt	179	$1/2^{\square}$	0.43	0.24				[6]
	181	$1/2^{\square}$	0.48	0.24				[6]
	183	$1/2^{\square}$	0.502	0.23	$7/2^{\square}$	0.78	0.24	[6]
	187	$3/2^{\square}$	-0.399	0.19				[5,79]
Os	189	3/2 1/2$^{\square}$ [510][(a)]	-0.32	~ 0.18[(b)]				[23,80]

(a) Excited state.

(b) From $B(E2)$ values of $^{188;190}$Os.

the $13/2^+$ state in ^{187}Pb at $E_{IS} = 33(13)$ keV above the $3/2^-$ ground state of ^{187}Pb. From this $E_{IS} = 33(13)$ keV value in ^{187}Pb we can deduce an energy location of the $13/2^+$ state in ^{183}Hg at $E_{IS} = 219(18)$ keV. This latter value is in better agreement with the value estimated from the systematics shown in fig. 10 than that given by the α decay of the ^{191}Po study. Furthermore, the 7336 keV α particles from ^{191}Po which served to locate the $13/2^+$ isomeric state in ^{187}Pb has a rather small HF value (HF = 21) for a $\Delta I = 5$ α transition with parity change (see table 6). Therefore, we have adopted the $E_{IS} = 33(13)$ keV value for the $13/2^+$ state in ^{187}Pb to determine the energy location of the $(13/2^+)$ isomeric states in the α-emitter chain starting with ^{195}Rn. Thus, the E_{IS} values obtained are 219(18) keV, 74(15) keV and 93(21) keV for the $13/2^+$ isomeric states in ^{183}Hg, ^{191}Po and ^{195}Rn, respectively.

It is well known that the main α decay of a nuclear state feeds preferably state with same spin value and same or close nuclear structure. Thus the results shown in fig. 9 and table 6 will be very useful to discuss the structure of some states of ^{185}Hg and ^{189}Pb nuclei in the next section.

5 Discussion

Before discussing the nuclear structure of the states of the ^{185}Hg and ^{189}Pb nuclei we have to recall what is known or well established in the neighbouring nuclei.

Important information on the isomeric and ground states of the Pt, Hg and Pb nuclei has been provided by laser spectroscopy experiments. Thus, nuclear deformation parameters, β, have been deduced from isotope shift measurements and, from hyperfine spectra, nuclear angular momenta, I, have been confirmed or determined. Furthermore, nuclear moments are determined from hyperfine spectra, the nuclear magnetic moments, μ, inform us about the structure of the nuclear states and, in some cases, the spectroscopic quadrupole moments, Qs, provide information on their nuclear shape. The β, I and μ values determined in that way for the isomeric and ground states of the nuclei of interest for the discussion are listed in table 7. All of the $1/2^-$ ground states listed in table 7 have similar μ values around $+0.48$ μ_N. This is in agreement with the $1/2^-[521]$ nuclear structure attributed to these ground states.

In their isomeric and ground states, the neutron-deficient semi-magical ^{187,189,191}Pb nuclei have a quasi-spherical shape since their β values are smaller than 0.1 (see table 7). The $13/2^+$ isomeric states of the Pb and Hg nuclei correspond to a neutron in the $i_{13/2}$ sub-shell, their μ values are similar and well reproduced by the theoretical calculations we have performed for spherical or weakly deformed prolate or oblate nuclear shape provided that the spin gyromagnetic factor used, g_s, is increased relatively to that of a free neutron, $g_{sfree} = -3.8$, to take into account polarization effects in nuclear surroundings. For weakly deformed nuclei, we have calculated the μ values using the semi-microscopic axial-rotor + 1 quasi-particle coupling model [81–83]. The μ values obtained for the ^{189}Pb $13/2^+$ isomeric state using $g_s = 0.6$ g_{sfree} are: $\mu = -1.15$ μ_N for spherical shape, $\mu = -1.16$ μ_N for weakly deformed prolate shape ($\beta = +0.08$) and $\mu = -1.23$ μ_N for weakly deformed oblate shape ($\beta = -0.07$). All of these calculated values are close to the measured value $\mu = -1.19$ μ_N.

On the other hand, the μ values of the $3/2^-$ ground states of the ^{187,189}Pb, ^{187}Hg and ^{187}Pt nuclei are all negative with values that increase rather quickly with the nuclear-deformation increase (see table 7). This is due to an increase of the configuration admixtures in the wave functions describing the $3/2^-$ states. For spherical nuclear shape if the neutron occupied the only $p_{3/2}$ sub-shell the μ value should be $\mu = -1.91$ μ_N for $g_s = g_{sfree}$ and $\mu = -1.15$ μ_N for $g_s = 0.6$ g_{sfree}. For a weakly deformed

prolate nuclear shape ($\beta = +0.08$) the wave function of the $3/2^-$ state of ^{189}Pb in spherical basis includes components corresponding to the coupling of the particle states ($p_{1/2}$, $p_{3/2}$, $f_{5/2}$, ...) with the excited states of the core (2^+, 4^+, ...). Thus, it becomes

$$\Phi = 0.27(p_{3/2}) + 0.23(2^+ \otimes p_{1/2}) + 0.13(2^+ \otimes p_{3/2}) + 0.11(4^+ \otimes f_{5/2}) + \ldots,$$

and the μ values calculated using $g_R = Z/A$ are

$$\mu = -0.66\ \mu_N \quad \text{for} \quad g_s = g_{sfree}$$

and

$$\mu = -0.22\ \mu_N \quad \text{for} \quad g_s = 0.6\ g_{sfree}.$$

In the same way, for a weakly deformed oblate nuclear shape ($\beta = -0.07$) the wave function of the $3/2^-$ state of ^{189}Pb becomes

$$\Phi = 0.53(p_{3/2}) + 0.27(2^+ \otimes p_{3/2}) + 0.13(2^+ \otimes f_{5/2}) + \ldots,$$

and the μ values calculated using the same g_R value are then

$$\mu = -0.81\ \mu_N \quad \text{for} \quad g_s = g_{sfree}$$

and

$$\mu = -0.43\ \mu_N \quad \text{for} \quad g_s = 0.6\ g_{sfree}.$$

Therefore, for the $3/2^-$ ground state of the ^{189}Pb nucleus the best agreement of the calculated μ value with that measured $\mu = -1.081\mu_N$ (see table 7) is obtained for a mainly $p_{3/2}$ configuration and a nuclear spherical shape.

The nuclear shape of the $3/2^-$ ground states of the weakly deformed ^{187,189,191}Pt and ^{187,189,191,193}Hg nuclei has been a much debated question. It has been shown that only the 3/2 1/2$^-$[510] Nilsson state corresponding to a prolate shape could explain the negative sign of both the Q_s and μ experimental values of these Pt and Hg $3/2^-$ ground states [79,83]. The μ value of the $3/2^-$ ground state of the ^{187}Pt nucleus is slightly smaller than that measured for the 3/2 1/2$^-$[510] Nilsson state known in ^{183}Os [23]. More recently, results obtained on the excited states of ^{187}Pt from in-beam experiments have confirmed the identification of the $3/2^-$ ground state of the ^{187}Pt nucleus as mainly the 3/2 1/2$^-$[510] Nilsson state corresponding to a prolate nuclear shape [84]. In a spherical basis, the main components of the wave function of the 3/2 1/2$^-$[510] state obviously correspond to the coupling of the 2^+ state of the core with the $f_{5/2}$ and $p_{3/2}$ particle states. Thus, the nuclear structure of the $3/2^-$ ground states of the ^{187,189}Pb, ^{187}Hg and ^{187}Pt nuclei varies rather slowly with the deformation increase, which explains the increase of the μ value of the $3/2^-$ ground state from neutron-deficient Pb to neutron-deficient Pt nuclei (see table 7).

Therefore, we know that the $3/2^-$ ground states of ^{187,189}Pb and ^{187}Hg have similar nuclear structure from their measured magnetic moments. In fig. 9 and table 6 we can see that the hindrance factors of the α transitions between the $3/2^-$ ground states ^{195,197,199}Rn $\rightarrow$ ^{191,193,195}Po $\rightarrow$ ^{187,189,191}Pb and ^{191}Pb $\rightarrow$ ^{187}Hg are small, $0.46 \leq$ HF ≤ 4, these favoured α transitions confirm that the $3/2^-$ ground states of these Rn, Po, Pb and ^{187}Hg nuclei have also similar nuclear structure. The $3/2^-$ ground state of the ^{187}Pb nucleus preferably decays towards the 275 keV level of the ^{183}Hg nucleus, HF = 2.2, which strongly suggests that the 275 keV level has a spin value $I = 3/2^-$ and a structure close to that of the $3/2^-$ ground state of ^{187,189,191}Pb, ^{187}Hg, ^{191,193,195}Po and ^{195,197,199}Rn nuclei. In ^{185}Hg, it is the 26 keV level that has a structure close to that of the $3/2^-$ ground state of the ^{189}Pb nucleus since the α decay of the $3/2^-$ ground state of ^{189}Pb is more favoured to the 26 keV level than to the 174 keV level in the ^{185}Hg nucleus. The 174 keV level of ^{185}Hg and the 67 keV level of ^{183}Hg probably have a structure that differs from that of the $3/2^-$ ground states of the Pb, Po and Rn nuclei. However, it is very probable that these 275, 67, 26 and 174 keV states correspond to a weak nuclear deformation of the ^{183,185}Hg nuclei.

From the μ values, we know that the structure of the 13/2 isomeric states of the ^{187,189,191}Pb and ^{185,187}Hg nuclei have a similar structure. The small hindrance factors, $0.9 \leq$ HF ≤ 3.4 determined for the α decay between the $13/2^+$ isomeric levels ^{197,199}Rn $\rightarrow$ ^{193,195}Po, ^{193,195}Po $\rightarrow$ ^{189,191}Pb, ^{189}Pb $\rightarrow$ ^{185}Hg and ^{187}Pb $\rightarrow$ ^{183}Hg indicate similar structure for these $13/2^+$ levels with a probable quasi-spherical nuclear shape. On the other hand, the structure of the $(13/2^+)$ isomeric state of the ^{191}Po nucleus probably differs from that of the $13/2^+$ isomeric states of these Pb nuclei since the hindrance factor of the α decay ^{191}Po $\rightarrow$ ^{187}Pb (first $13/2^+$) is rather high, HF = 70. It is rather close to that of both the second $(13/2^+)$ level of the ^{187}Pb nucleus and $(13/2^+)$ isomeric state of the ^{195}Rn nucleus. It is worth noting that, from different theoretical approaches, an increase of the nuclear deformation has been predicted to arise in the neutron-deficient even-even Po. For example, May **et al.** [85] predict this deformation increase between ^{190}Po ($\beta = 0.21$) and ^{188}Po ($\beta = 0.28$) and more recently, Delaroche **et al.** [86] predict it between ^{192}Po ($\beta = 0.21$) and ^{190}Po ($\beta = 0.29$). Therefore, the structure change observed for the isomeric state between ^{193}Po and ^{191}Po indicates that the isomeric states in ^{191}Po and ^{195}Rn could correspond to a well-deformed prolate nuclear shape. In that case the two isomeric states would probably have a spin value that differs from the 13/2 proposed in the literature.

6 Conclusion

The study of the ^{185}Tl decay performed in this work has served to identify about fifty γ-rays belonging to the β^+/EC decay of the $1/2^+$ ground state of the ^{185}Tl nucleus towards levels of the ^{185}Hg nucleus. It has also confirmed that the $9/2^-$ isomeric state of ^{185}Tl decays by a cascade of two isomeric transitions (fig. 2) whereas its β^+/EC decay was not observed. Furthermore, for the first time, a partial level scheme of low-spin levels ($I < 9/2$) of the ^{185}Hg nucleus has been built.

Conversion electron lines of very low-energy transitions $8 < E < 36$ keV were observed for the first time thanks to measurements performed using the VLECED setup. The electron data have been obtained for six transitions, four in ^{185}Au and two in ^{185}Hg. The analysis of the high energy resolution electron spectrum using an internal calibration has allowed us to precisely determine the energies of one transition in ^{185}Au and two of the three isomeric transitions of ^{185}Hg. Thus, the energy location of the $13/2^+$ isomeric state of ^{185}Hg has been determined to be $E_{\rm is} = 103.7(4)$ keV. By combining the known α-decay results of the ^{185}Hg nucleus with the well-known level scheme of the ^{181}Pt nucleus we have estimated an independent value for the excitation energy of the $13/2^+$ isomeric state in ^{185}Hg, $E_{\rm is} = 94(13)$ keV. Both values are in agreement. Our value $E_{\rm is} = 103.7(4)$ keV would be also in reasonable agreement with the value deduced from the ISOLTRAP experiment [35] provided an unexpected systematic error of 20 keV is added to the statistic error, which would give $E_{\rm is} = 120(21)$ keV instead of $E_{\rm is} = 120(5)$ keV.

The origin of the three α lines emitted from the two ^{189}Pb isomers has been unambiguously identified from the hyperfine spectrum observed for each α line. This, combined with the α-γ coincidence measurement, the identification of the γ-rays from the β^+/EC decay of the $1/2^+$ ground state of the ^{185}Tl nucleus and the energy location of the $13/2^+$ isomeric state in ^{185}Hg has allowed us to locate the $13/2^+$ isomeric state at 40(4) keV above the $3/2^-$ ground state of the ^{189}Pb nucleus. Furthermore, using known α-decay data, the $13/2^+$ isomeric states have been located at 95(7) keV and 194(12) keV above the $3/2^-$ ground states of the ^{193}Po and ^{197}Rn nuclei, respectively.

The comparison of the properties of the nuclei of the three α-emitter chains starting with the ^{195,197,199}Rn nuclei strongly suggests that the $3/2^-$ excited states at 26 keV in ^{185}Hg and at 275 keV in ^{183}Hg have a nuclear structure similar to that (mainly $p_{3/2}$) of the $3/2^-$ ground states of the ^{187}Hg, ^{187,189,191}Pb, ^{191,193,195}Po and ^{195,197,199}Rn nuclei that have spherical or weakly deformed prolate shape. In the same way, the nuclear structure of the $13/2^+$ isomeric states of the ^{191}Po and ^{195}Rn nuclei that appears to be similar to that of the second $13/2^+$ state of ^{187}Pb, differs from that of the other $13/2^+$ isomeric states that correspond to a $i_{13/2}$ structure with quasi-spherical nuclear shape. The structure change of the isomeric state observed between ^{193}Po and ^{191}Po could be due to a large increase of the nuclear deformation for the isomeric state between ^{193}Po and ^{191}Po.

We acknowledge support from the Spanish MINECO through projects FPA2010-17142 and CPAN CSD-2007-00042.

Open Access This is an open access article distributed under the terms of the Creative Commons Attribution License (http://creativecommons.org/licenses/by/3.0), which permits unrestricted use, distribution, and reproduction in any medium, provided the original work is properly cited.

References

1. G. Ulm **et al.**, Z. Phys. A **325**, 247 (1986) and references therein.
2. R. Beraud **et al.**, Nucl. Phys. A **284**, 221 (1977) and references therein.
3. K. Wallmeroth **et al.**, Nucl. Phys. A **493**, 224 (1989).
4. G. Savard **et al.**, Nucl. Phys. A **512**, 241 (1990).
5. T. Hilberath **et al.**, Z. Phys. A **342**, 1 (1992).
6. F. Le Blanc **et al.**, Phys. Rev. C **60**, 054310 (1999).
7. D. Verney **et al.**, Eur. Phys. J. A **30**, 489 (2006).
8. K. Heyde, P. van Isacker, M. Waroquier, J.L. Wood, R.A. Meyer, Phys. Rep. **102**, 291 (1983) and references therein.
9. J.L. Wood, K. Heyde, W. Nazarewicz, M. Huyse, P. Van Duppen, Phys. Rep. **215**, 101 (1992) and references therein.
10. K. Heyde, J.L. Wood, Rev. Mod. Phys. **83**, 1467 (2011) and references therein.
11. H. de Witte **et al.**, Phys. Rev. Lett. **98**, 112502 (2007).
12. M. Seliverstov **et al.**, Eur. Phys. J. A **41**, 315 (2009).
13. P. Kilcher **et al.**, Nucl. Instrum. Methods A **274**, 485 (1989).
14. P. Kilcher **et al.**, AIP Conf. Proc. **164**, 517 (1987).
15. G.W. Grüter, B. Jonson, O.B. Nielsen, 3rd International Conference on Nuclei far from Stability, Cargese, June 1976, Proc. CERN 76-13, 428 (1976).
16. M.J.A. de Voigt **et al.**, Nucl. Phys. A **507**, 447 (1990).
17. J. Sauvage **et al.**, Nucl. Phys. A **540**, 83 (1992).
18. E. Kugler **et al.**, Nucl. Instrum. Methods B **70**, 41 (1992).
19. S. Du, O. Hubert, J. Le Bris, R. Sellem, IPNO Report (1998-1999) Technical Activities, p. 110.
20. J. Le Bris **et al.**, Rapport interne IPNO 06-03 (English version).
21. J. Le Bris **et al.**, Rapport interne IPNO 05-04 (French version).
22. A.G. Schmidt **et al.**, Phys. Lett. B **66**, 133 (1977).
23. Richard B. Firestone, Virginia S. Shirley, Table of Isotopes, 8th edition (John Wiley & Sons Inc., New York, 1996).
24. C. Bourgeois, P. Kilcher, B. Roussière, J. Sauvage-Letessier, M.G. Porquet, Nucl. Phys. A **386**, 308 (1982).
25. P. Paris **et al.**, Nucl. Instrum. Methods **186**, 91 (1981).
26. J.C. Putaux **et al.**, Nucl. Instrum. Methods **186**, 321 (1981).
27. J. Sauvage **et al.**, Proc. TRIUMF-ISOL Workshop, Mont Gabriel, Québec, Canada, TRI-84-1 (1984) p. 161.
28. B. Roussière **et al.**, Nucl. Phys. A **643**, 331 (1998).
29. F.P. Larkins, At. Data Nucl. Data Tables **20**, 311 (1977).
30. M.H. Chen, B. Crasemann, H. Mark, At. Data Nucl. Data Tables **24**, 13 (1979).
31. P.G. Hansen **et al.**, Nucl. Phys. A **148**, 249 (1970).
32. E. Hagberg, P.G. Hansen, P. Hornshøj, B. Jonson, S. Mattsson, P. Tidemand-Petersson, Nucl. Phys. A **318**, 29 (1979).
33. S.-C. Wu, Nucl. Data Sheets **106**, 367 (2005).
34. S.-C. Wu, Nucl. Data Sheets **106**, 619 (2005).
35. S. Schwarz **et al.**, Nucl. Phys. A **693**, 533 (2001).
36. J. Lettry **et al.**, Rev. Sci. Instrum. **69**, 761 (1998).
37. U. Köster **et al.**, Nucl. Instrum. Methods B **204**, 347 (2003).
38. R. Dissert, H. Friedmann, M. Klipfel, A. Krauth, R. Limbach, G. Walter, CRN report (1990) ISBN 0755-3404, p. 156.
39. J. Sauvage **et al.**, Eur. Phys. J. A **39**, 33 (2009).

40. H. Gauvin, Y. Le Beyec, M. Lefort, N.T. Porile, Phys. Rev. Lett. **29**, 958 (1972).
41. P. Hornshøj et al., Nucl. Phys. A **230**, 365 (1974).
42. J.O. Rasmussen, alpha-, beta- and gamma-ray spectroscopy, edited by Kai Siegbahn, Vol. **1** (North Holland Publishing Company, Amsterdam, 1965) Ch. XI, p. 701.
43. Zhou Chumei, Nucl. Data Sheets **86**, 645 (1999).
44. C. Di Rienzo et al., Phys. Rev. C **21**, 2101 (1980).
45. F. Calaprice, G.T. Ewan, Phys. Rev. C **30**, 1671 (1984).
46. H.E. Enge et al., Phys. Rev. C **24**, 298 (1981).
47. J. Wauters et al., Phys. Rev. C **47**, 1447 (1993).
48. E. Achterberg et al., Nucl. Data Sheets **107**, 1 (2006).
49. T. Enqvist et al., Z. Phys. A **354**, 9 (1996).
50. V.R. Vanin et al., Nucl. Data Sheets **108**, 2393 (2007).
51. H. Kettunen et al., Phys. Rev. C **63**, 044315 (2001).
52. T.E. Cocolios et al., J. Phys. G Nucl. Part. Phys. **37**, 125103 (2010) and references therein.
53. A.N. Andreyev et al., AIP Conf. Proc. **495**, 121 (1999).
54. S.-C. Wu, H. Niu, Nucl. Data Sheets **100**, 1 (2003).
55. S. Della Negra, B. Lagarde, Y. Le Beyec, J. Phys. Lett. **38**, L393 (1977).
56. M.E. Leino, S. Yashita, A. Ghiorso, Phys. Rev. C **24**, 2370 (1981).
57. M.S. Basunia, Nucl. Data Sheets **110**, 299 (2009).
58. J.C. Batchelder et al., Phys. Rev. C **55**, R 2142 (1997).
59. A.N. Andreyev et al., Phys. Rev. Lett. **82**, 1819 (1999).
60. A.N. Andreyev et al., Phys. Rev. C **66**, 014313 (2002).
61. Y. Le Beyec, M. Lefort, J. Livet, N.T. Porile, Phys. Rev. C **9**, 1091 (1974).
62. Coral M. Baglin, Nucl. Data Sheets **91**, 117 (2009).
63. P. Misaelides et al., Z. Phys. A **301**, 199 (1981).
64. Coral M. Baglin, Nucl. Data Sheets **110**, 265 (2009).
65. M.I. Macias-Marques et al., Nucl. Phys. A **427**, 205 (1984).
66. M.G. Desthuilliers et al., Nucl. Phys. A **313**, 221 (1979).
67. W.F. Mueller et al., Phys. Rev. C **59**, 2009 (1999).
68. G.J. Lane et al., Nucl. Phys. A **589**, 129 (1995).
69. D.T. Shi et al., Phys. Rev. C **51**, 1720 (1995).
70. B. Roussière et al., Proceedings of the International Symposium on In-Beam Nuclear Spectroscopy, Debrecen, Hungary (1984).
71. F. Hannachi et al., Z. Phys. A **330**, 15 (1988).
72. G.D. Dracoulis, C. Fahlander, A.P. Byrne, Nucl. Phys. A **401**, 490 (1983).
73. A. Neskakis et al., Nucl. Phys. A **261**, 189 (1976).
74. B. Roussière et al., Z. Phys. A **351**, 127 (1995).
75. B. Roussière, C. Bourgeois, P. Kilcher, J. Sauvage, M.G. Porquet, Nucl. Phys. A **504**, 511 (1989).
76. J. Nyberg et al., Nucl. Phys. A **511**, 92 (1990).
77. C. Weber et al., Phys. Lett. A **347**, 81 (2005).
78. S.B. Dutta et al., Z. Phys. A **341**, 39 (1991).
79. J. Sauvage et al., Hyperfine Interact. **129**, 303 (2000).
80. S. Raman et al., At. Data Nucl. Data Tables **36**, 26 (1987).
81. M. Meyer et al., Nucl. Phys. A **316**, 93 (1979).
82. J. Libert et al., Phys. Rev. C **25**, 582 (1982).
83. J. Sauvage et al., Phys. At. Nucl. **64**, 1134 (2001).
84. D. Hojman et al., Eur. Phys. J. A **48**, 83 (2012).
85. F.R. May, V.V. Pashkevich, S. Frauendorf, Phys. Lett. B **68**, 113 (1977).
86. J.P. Delaroche et al., Phys. Rev. C **81**, 014303 (2010) and `http://www-phynu.cea.fr/HFB-5DCH-table.htm`.